

The Crystal and Molecular Structures of the Diastereomeric (4*Z*)- and (4*E*)-3-Oxo-2,3-dihydrobilatrienes-abc**

Christoph Kratky^{a,*}, Heinz Falk^b, and Karl Grubmayr^b

^a Institut für Physikalische Chemie, Universität Graz, A-8010 Graz, Austria

^b Institut für Analytische, Organische und Physikalische Chemie, Johannes-Kepler-Universität Linz, A-4040 Linz, Austria

(Received 13 June 1984. Accepted 12 July 1984)

The molecular and crystal structures of two diastereomeric 3-oxo-2,3-dihydrobilatrienes-abc **1** and **2** are determined at low (**1**, **2**) and room temperature (**2**). The configurations at the exocyclic double bond in position 4 are found to be (*Z*) for **1** and (*E*) for **2**. Tautomerism, conformation and crystal packing of **1** and **2** can be understood on the basis of the pattern of intra- and intermolecular hydrogen bonds. Compared to **1**, a more open helix conformation is found for the (*E*) diastereomer **2**. An analysis of crystallographically observed temperature factors of **2** yields the result that the highest flexibility is found for the saturated lactam ring.

(Keywords: Crystal structure of 3-oxo-2,3-dihydrobilatriene-abc; Dihydrobilatriene-abc; 3-oxo-2,3-dihydrobilatriene-abc; Phytochrome model compounds)

*Die Kristall- und Molekülstruktur zweier diastereomerer (4*Z*)- und (4*E*)-3-Oxo-2,3-dihydrobilatriene-abc*

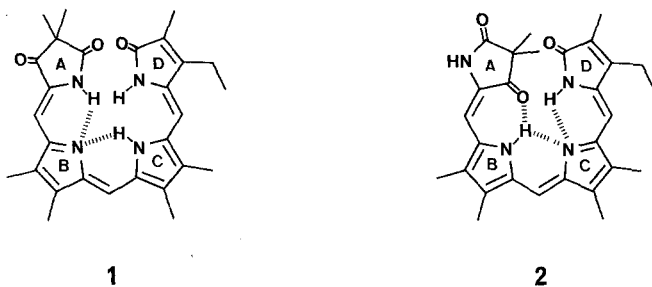
Die Molekül- und Kristallstruktur zweier diastereomerer 3-Oxo-2,3-dihydrobilatriene-abc **1** und **2** wurde bei tiefer Temperatur (**1**, **2**) und Raumtemperatur (**2**) bestimmt. Die Konfiguration an der exocyclischen Doppelbindung in Position 4 von **1** wird als (*Z*), von **2** als (*E*) gefunden. Tautomerie, Konformation und Kristallpackung werden auf Grund der intra- und intermolekularen Wasserstoffbrückenbindungen verständlich. Eine gegenüber **1** aufgeweitete Helixkonformation wird für das (*E*)-Diastereomere **2** gefunden. Aus einer Analyse der kristallographisch beobachteten Temperaturkoeffizienten von **2** wird auf eine ausgeprägte Flexibilität des gesättigten Laktamringes geschlossen.

** Herrn Prof. Josef Schurz zum 60. Geburtstag gewidmet.

Introduction

A key to the understanding of the phototransformation of phytochrome are possible derivatives of photoreactions on the chromophore molecule, which is known to be a 2,3-dihydrobilatriene-*abc*¹. An important group of such photoreaction products are diastereomers with respect to the configuration about one of the exocyclic double bonds^{1,2}.

Thermodynamically, the (*Z, Z, Z*) configuration is preferred for most dihydrobilatrienes-*abc*. However, there are various ways to make (*E*)-configured diastereomers accessible; one way is by means of a hydrogen-bond acceptor in position 3, which stabilizes the (*5E*)-isomer through intramolecular H-bonds to the pyrrole protons of the adjacent rings². Such a situation exists in compounds **1** and **2**.



In the preceding communication³ we reported the crystal structures of a pair of (*Z*) and (*E*) diastereomers of a dihydropyrromethenone system. Here, we describe the results of crystal structure analyses on compounds **1** and **2**. To our knowledge, they are the first structure determinations on linear tetrapyrroles of the 2,3-dihydrobilatriene-*abc* type, and the crystal structure of **2** yields the first example of a linear tetrapyrrole with (*E*)-configuration about one of the exocyclic double bonds. The relevance of the present work is corroborated by the close structural resemblance of **1** and **2** not only to phytychromobilin¹, but also to phycocyanobilin, the chromophore molecule isolated from the accessory pigment phycocyanine⁴.

To attain optimum accuracy, both structures were determined at low temperature. The structure of **2** was also determined at room temperature. Comparison of the two data sets of **2** allows the detection of disordered atoms in the crystal. Finally, we will present the result of an analysis of the temperature factors to obtain an indication about the molecular flexibility in the crystal, following the method outlined in the preceding communication³.

Experimental

Crystals of **1**² were obtained from pyridine/ethanol: about 0.5 ml of a concentrated solution of **1** in pyridine was left in an open beaker inside a dessiccator, which contained a second open vessel with ethanol. Crystals suitable for structure determination appeared after several months in the cold room. Under the same crystallization conditions, compound **2**² yielded triclinic crystals [room temperature cell constants: $a = 8.41$, $b = 11.63$, $c = 14.16$ Å, $\alpha = 109.46^\circ$, $\beta = 93.90^\circ$, $\gamma = 96.310^\circ$, $V = 1291$ Å³, d_x (for $C_{28}H_{32}N_4O_3$, $Z = 2$) = 1.21 gcm⁻³],

Table 1. Summary of experimental conditions

	1 (low temp.)	2 (low temp.)	2 (room temp.)
chemical formula	$C_{28}H_{32}N_4O_3$	$C_{28}H_{32}N_4O_3 \cdot CHCl_3$	
crystal size [mm]	$.3 \times .06 \times .3$	$.1 \times .15 \times .25$	$.1 \times .25 \times .25$
temperature [K] (cold stream)	103 ± 3	90 ± 1	293 ± 2
space group	$P\bar{1}$		$P\bar{1}$
cell dimensions			
a [Å]	9.453 (2)	9.657 (2)	9.864 (1)
b [Å]	11.540 (4)	11.396 (1)	11.594 (1)
c [Å]	12.969 (1)	14.230 (3)	14.243 (3)
α [°]	108.04 (2)	80.44 (1)	80.96 (1)
β [°]	96.22 (1)	70.89 (1)	70.40 (1)
γ [°]	105.36 (2)	84.24 (1)	84.54 (1)
V [Å ³]	1268.9	1457.4	1513.9
number of molecules per unit cell	2		2
calculated density [gcm ⁻³]	1.237	1.349	1.299
number and θ -range [°] of reflections used to refine cell constants	18 $12 \leq 2\theta \leq 21$	13 $24 \leq 2\theta \leq 28$	24 $17 \leq 2\theta \leq 21$
limits for data collection [°]	$0 \leq 2\theta \leq 50$ $-11 \leq h \leq 11$ $-13 \leq k \leq 13$ $0 \leq l \leq 15$	$0 \leq 2\theta \leq 60$ $-13 \leq h \leq 13$ $-16 \leq k \leq 16$ $0 \leq l \leq 20$	$0 \leq 2\theta \leq 50$ $-11 \leq h \leq 11$ $-13 \leq k \leq 13$ $0 \leq l \leq 16$
scan type/scan width [°]	$\omega/0.8$	$\omega\text{-}\theta/1.1$	$\omega\text{-}\theta/1.0$
number/frequency of standard refs.	3/60	3/100	3/100
max. variation of standard intensities	$\pm 15\%$	$\pm 3\%$	-17%
number of observed reflections	4928	9072	5721
number of independent reflections	4454	8486	5262
number of reflections with $ F_o > 4\sigma(F_o)$	1262	3508	1668
R/R _w -factors	.066/.060	0.056/0.049	0.057/0.055
number of parameters	329	484	394
number of observations (including distance constraints)	1288	3534	1668
coefficients a/b of weighting system $w_i = a/(\sigma^2(F_i) + bF_i^2)$	1/0	1/0	2.6/0.0001
highest peak/lowest trough in final ΔF -Fourier synthesis [e Å ⁻³]	0.30/-0.31	0.46/-0.42	0.28/-0.24

which unfortunately were unsuitable for data collection due to twinning. Eventually, suitable crystals of **2** were obtained from chloroform/*n*-hexane, using the above method (material dissolved in chloroform, kept in the coldroom for several weeks).

A locally modified STOE 4-circle diffractometer (MoK α -radiation, graphite monochromator, $\lambda = 0.71069 \text{ \AA}$) equipped with a NONIUS low temperature attachment was used for the subsequent X-ray work. To prevent ice-deposition on the crystal, the whole diffractometer was placed inside a glove box. Relevant experimental conditions and a summary of the results of structure refinement are given in Table 1.

During collection of the low temperature intensity data for compound **1**, we observed long-term (several hours) fluctuations of the three periodically re-measured standard intensities ($\pm 15\%$). These fluctuations, which affected all three standard intensities by about the same factor, had no obvious explanation, until—several months later—it was found that the current-stabilization of the X-ray generator was defective. Since long-term fluctuations can reasonably well be corrected from standard intensities, we did not remeasure the data set.

The standard intensities for the room temperature data of **2**—which were collected after repair of the above defect—showed a continuous and more-or-less parallel decrease by a total of 17%, which must be ascribed to decomposition of the crystal (possibly partial loss of the solvated chloroform).

Data reduction involved a correction for the above effects (application of a scale factor derived from the standard intensities), merging of multiply recorded and symmetry related reflections and LP correction. Neither absorption nor extinction corrections were applied [μ (MoK α) = 0.88 cm $^{-1}$ for **1** and 3.5 cm $^{-1}$ for **2**]. The structures were solved by direct methods and refined by least-squares.

Refinement (which had to be carried out in a blocked mode due to computer limitations) differed somewhat between the three data sets. For the low temperature structure of **1**, atoms C 1 to N 23 were refined with isotropic, atoms O 24–O 35 with anisotropic temperature coefficients. Hydrogen atoms were also refined (isotropic temperature factors), for H-atoms bonded to sp 3 -carbons, the bonding distance was constrained to 1.09 Å. For the low temperature structure of **2**, all non-H atoms were refined with anisotropic temperature coefficients, hydrogens were treated as in **1**. Refinement of the room temperature data of **2** started from the final low temperature coordinates; H-atoms bonded to carbon were kept at their low temperature coordinates (only isotropic temperature factors refined), non-H atoms were subjected to unconstrained, anisotropic refinement. The positions for the three H-atoms bonded to nitrogen (H 20, H 21, H 23) were also refined. Computer programs are given in Ref.⁵.

Results and Discussion

Tables 2 to 5 give atomic coordinates and temperature coefficients for both low-temperature structures (**1** and **2**) and for the room-temperature structure of **2**. Compared to most other crystal structures of linear tetrapyrroles⁶, the structures are of unusual quality, which is illustrated by the successful localization and refinement of hydrogen atom positions. This is particularly important for the H-atoms involved in hydrogen bonding, since the pattern of intra- and intermolecular H-bonds is crucial for conformation and crystal packing in both compounds. The following

Table 2. Atomic coordinates and (equivalent) isotropic temperature factors ($\cdot 10^4$, U -values in \AA^2) for the low temperature crystal structures of **1** (right) and **2** (left). E.s.d.'s are given in italics. The equivalent isotropic temperature factor was obtained as one third of the trace of the orthogonalized U_{ij} tensor, and it corresponds to a temperature factor of the form $T = \exp(-8\pi^2 \cdot U \cdot \sin^2 \vartheta / \lambda^2)$

Atom	X/a	Y/b	Z/c	U _{iso}	X/a	Y/b	Z/c	U _{iso}
C1	10047 4	7194 3	-979 3	206 24	9532 10	8126 8	11434 7	363 24
C2	9140 4	7926 3	-162 3	150 21	11021 10	8993 8	12191 7	327 24
C3	8017 4	7039 3	534 3	145 21	12119 10	9015 8	11447 7	348 23
C4	8182 4	5989 3	41 3	147 21	11250 10	8311 8	10293 7	333 24
C5	7343 4	5017 3	252 3	154 21	11798 11	8290 9	9389 8	314 25
C6	6064 4	4682 3	1075 3	144 21	10981 10	7872 8	8244 7	335 24
C7	5162 4	3741 3	1158 3	183 22	11519 9	7923 8	7304 7	267 22
C8	4017 4	3753 3	2056 3	182 22	10430 9	7144 8	6391 7	271 21
C9	4218 4	4682 3	2535 3	171 21	9280 9	6396 8	6784 7	257 22
C10	3383 4	5032 4	3467 3	203 23	8053 10	5388 9	6123 8	326 23
C11	3748 4	5759 3	4011 3	180 22	8979 9	4504 8	6404 7	277 22
C12	2848 4	6158 4	4953 3	216 23	5689 10	3513 8	5764 7	308 23
C13	3705 4	6798 4	5239 3	238 24	4998 9	2953 8	6484 7	292 23
C14	5136 4	6796 3	4461 3	179 22	5885 10	3606 8	7559 7	353 24
C15	6418 5	7360 4	4471 3	223 24	5524 10	3399 8	8533 7	308 23
C16	7776 4	7201 3	3810 3	178 23	6412 9	3904 8	9567 7	265 22
C17	9155 4	7728 3	3694 3	197 24	5979 9	3907 8	10614 7	255 21
C18	10218 4	7308 3	2926 3	182 23	7196 9	4578 8	11448 7	300 23
C19	9557 4	6455 3	2528 3	172 22	8476 9	4978 8	10948 7	274 22
N20	9433 3	6131 3	-826 2	178 18	9774 8	7761 7	10343 6	320 19
N21	5473 3	5227 3	1919 2	165 19	9646 7	6770 6	7938 5	262 18
N22	5162 3	6195 3	3727 2	188 18	7085 8	4525 7	7483 6	288 20
N23	8100 3	6454 3	3083 2	171 19	7969 9	4596 7	9831 6	291 21
O24	11141 3	7527 3	-1675 2	347 20	8333 7	7774 6	6 11870 5	444 50
C25	8331 5	8958 4	-826 3	220 25	11434 13	8500 12	13139 9	515 89
C26	10083 4	8359 4	363 3	199 24	10894 14	10347 11	12709 10	578 95
O27	7128 3	7238 2	1333 2	177 15	13486 7	9528 7	11737 5	533 53
C28	5448 5	2894 4	407 3	220 25	12934 12	8969 10	7389 9	408 80
C29	2773 5	2920 4	2493 3	255 26	10410 11	7103 10	5219 8	368 78
C30	1263 5	5914 4	5458 3	268 27	5133 13	3154 11	4534 8	458 87
C31	3379 5	7393 4	6158 3	311 29	3563 12	1844 11	6117 9	455 78
C32	9295 5	8619 4	4335 3	293 29	4405 11	3311 9	10699 7	297 68
C33	9072 11	9873 5	3907 6	823 67	4021 13	1848 10	10435 11	497 94
C34	11779 5	7601 4	2463 3	241 26	7332 11	4950 10	12679 8	338 75
O35	10165 3	5847 2	1854 2	217 16	9825 6	5537 5	11438 5	331 44
C36*	4591 4	806 4	7567 3	232 24				
CL37*	5344 1	451 1	8565 1	306 7				
CL38*	3211 1	-419 1	7855 1	284 6				
CL39*	5989 1	362 1	6439 1	353 7				

discussion will mainly be based on the two low temperature structures, which are superior in accuracy to the room temperature structure of **2**. Fig. 1 gives the intramolecular bonding geometry for the non-H atoms and the acidic protons, as observed in the low temperature crystal structures, and it defines the atom numbering used for the description of the crystal structures.

Table 3. Coordinates and isotropic temperature factors ($\cdot 10^3$) for the H-atoms in the low temperature crystal structures of **1** (right) and **2** (left). Note that positional E.s.d.'s may be underestimated due to distance constraints (see text in experimental section)

Atom	X/a	Y/b	Z/c	\bar{U}_{iso}	X/a	Y/b	Z/c	\bar{U}_{iso}								
H -C5	766	4	452	3	-24	3	22	11	1276	15	859	12	936	11	68	58
H -C10	253	4	470	3	379	3	14	10	791	6	525	5	531	5	0	16
H -C15	623	3	790	3	496	3	5	9	429	10	279	8	850	7	56	28
H -N20	971	3	559	3	-125	2	0	8	894	7	715	6	963	5	18	18
H -N21	582	4	587	3	195	3	20	11	776	9	499	8	798	7	43	26
H -N23	758	3	599	3	301	2	4	9	854	9	451	7	954	7	43	28
H1 -C25	905	3	953	3	-124	2	29	11	1060	8	870	9	1364	6	88	35
H2 -C25	760	3	941	3	-3	2	34	12	1255	4	909	6	1364	6	40	26
H3 -C25	771	4	868	4	-105	3	41	13	1156	9	756	4	1275	6	35	25
H1 -C26	1074	3	764	2	62	2	8	9	1031	11	1010	11	1334	6	115	44
H2 -C26	943	4	877	3	102	2	29	11	1047	12	1061	10	1203	6	114	38
H3 -C26	1087	3	897	3	-16	2	37	13	1198	5	1104	8	1318	7	128	41
H1 -C28	454	4	232	4	60	4	71	17	1394	6	903	8	793	6	85	30
H2 -C28	553	4	338	3	-33	1	32	11	1282	8	992	3	779	6	14	23
H3 -C28	643	3	234	3	40	4	68	15	1328	9	889	8	660	4	61	29
H1 -C29	262	6	264	5	329	1	98	21	1041	8	616	3	470	5	37	22
H2 -C29	204	5	305	5	204	4	94	20	1144	7	767	8	508	8	91	38
H3 -C29	298	5	202	2	230	4	67	16	942	5	732	8	492	7	33	28
H1 -C30	97	5	610	4	622	1	44	14	580	13	378	10	416	10	154	54
H2 -C30	60	4	648	3	506	3	46	13	439	10	361	10	423	9	122	41
H3 -C30	110	4	510	4	541	3	24	12	490	12	225	11	417	9	82	42
H1 -C31	367	4	831	1	606	3	36	12	289	8	169	8	672	6	64	29
H2 -C31	224	2	739	4	663	3	70	16	377	11	93	5	595	8	74	35
H3 -C31	394	4	693	4	667	3	52	15	281	13	170	15	532	9	186	69
H1 -C32	866	4	838	4	512	1	60	16	420	9	381	6	1150	3	43	25
H2 -C32	1039	2	849	4	441	3	31	12	354	8	339	9	1012	6	60	34
H1 -C33	808	5	1018	7	372	6	169	37	297	7	167	10	1072	9	121	41
H2 -C33	982	3	1015	3	317	2	38	9	477	5	158	5	1095	4	29	17
H3 -C33	921	5	1056	3	432	3	63	17	439	7	140	6	968	3	16	21
H1 -C34	1199	4	829	2	182	2	31	11	625	4	459	6	1268	6	17	22
H2 -C34	1245	3	686	2	213	3	20	10	787	9	599	2	1301	7	81	31
H3 -C34	1225	4	786	4	299	2	36	13	800	8	450	7	1306	6	55	28
H -C36*	411	5	147	4	750	3	37	13								

Molecular Constitution and Conformation

Fig. 2 and 3 show ORTEP-drawings of **1** and **2**, projected into a mean plane through the molecules. Evidently, both molecules are in more or less helical conformations. Some of the differences between the two diastereomers become apparent from Fig. 4, which shows an "edge on" projection for both molecules; the obviously more "open" conformation of **2** is also reflected in the six torsion angles (Fig. 1): while in **1**, the main twist occurs between rings A and B and between C and D (with rings B and C approximately coplanar), in **2** the largest twist angles are observed between rings C and D. The sum of the six torsion angles is 47° in **1** and 43°

Table 4. Result of the refinement of **2** against the room temperature data

Atom	X/a	Y/b	Z/c	U _{iso}
C1	9994 10	7169 8	-1019 8	652 76
C2	9144 9	7887 7	-210 7	502 67
C3	8038 8	7036 7	509 7	454 64
C4	8184 9	5984 8	49 7	492 63
C5	7351 9	5026 7	251 7	505 68
C6	6108 9	4711 7	1084 7	459 64
C7	5196 9	3789 7	1182 8	519 71
C8	4096 11	3839 7	2087 8	579 77
C9	4323 10	4735 8	2538 8	575 73
C10	3496 9	5093 8	3472 9	602 78
C11	3864 10	5810 8	4012 8	595 70
C12	2974 11	6236 9	4958 9	683 79
C13	3832 13	6851 9	5231 8	704 82
C14	5230 11	6822 8	4441 8	612 77
C15	6448 13	7373 9	4465 7	672 85
C16	7785 11	7224 7	3807 7	576 75
C17	9182 12	7739 8	3698 8	575 80
C18	10219 10	7302 8	2929 7	550 72
C19	9581 10	6464 7	2540 7	557 71
N20	9398 7	6134 6	-845 5	555 53
H-N20	9657 60	5652 46	-1209 46	133 198
N21	5554 6	5251 6	1917 5	509 48
H-N21	5845 75	5875 60	2002 59	717 284
N22	5251 6	6229 5	3717 4	567 46
N23	8150 7	6470 5	3085 5	540 50
H-N23	7540 64	6088 52	2944 50	587 228
O24	11062 7	7482 5	-1720 5	1118 53
C25	8357 9	8919 7	-834 7	687 69
C26	10098 8	8299 7	307 6	619 59
O27	7172 5	7235 4	1312 4	576 36
C28	5451 8	2959 7	439 7	657 66
C29	2846 9	3033 8	2503 8	880 82
C30	1407 9	6006 9	5469 8	948 82
C31	3479 12	7454 10	6146 7	1062 96
C32	9305 10	8629 8	4314 7	822 83
C33	9137 16	9823 10	3879 11	1388 146
C34	11766 9	7581 7	2488 7	707 71
O35	10180 5	5865 4	1863 4	693 41
C36*	4622 11	629 9	7580 8	661 81
CL37*	5316 3	439 3	6581 3	1032 28
CL38*	3229 3	-334 3	7851 3	1011 27
CL39*	5980 4	367 3	6473 3	1128 28

in **2**, the sum of the square of the torsion angles is 590 deg² in **1** and 370 deg² **2**; naively, one might conclude that there is less torsional strain energy in the more "open" conformation of **2**, which appears to be enforced by the steric repulsion between rings A (atoms C 26, O 27, C 3) and D (N 23, C 19, O 35); the five shortest contact distances are: O 27 - N 23, 2.92; C 26 - O 35, 3.27; C 3 - O 35, 3.29; O 27 - C 19, 3.30; C 26 - C 19, 3.38 Å.

Table 5. Anisotropic temperature coefficients ($\cdot 10^4$, in \AA^2) for the non-H atoms in the low-temperature structure of **2**. The temperature factor has the form:

$$T = \exp(-2\pi^2(h^2 a^{*2} u_{11} + \dots + 2hka^* b^* u_{12} + \dots))$$

Atom	u11	u22	u33	u12	u13	u23
C1	242 22	207 22	161 21	-64 17	-24 17	-55 17
C2	190 20	146 19	115 19	-75 16	-25 16	-28 15
C3	190 20	120 19	134 19	-22 15	-67 16	-6 15
C4	179 20	143 19	111 19	0 16	-41 16	-11 15
C5	158 19	121 19	188 21	12 15	-62 17	-36 16
C6	156 19	112 18	172 20	-2 15	-60 16	-28 16
C7	172 20	133 19	248 23	9 16	-83 17	-15 17
C8	171 20	136 20	237 22	-35 16	-75 17	14 17
C9	139 19	159 19	198 21	-9 15	-56 16	25 16
C10	93 19	228 22	231 22	-33 17	-3 17	40 18
C11	170 20	198 21	136 20	0 17	-24 16	11 17
C12	170 21	239 22	150 21	82 17	20 17	17 17
C13	253 22	247 23	148 21	97 18	-16 18	-10 18
C14	176 20	156 20	160 20	35 16	-20 16	0 16
C15	312 24	213 22	145 21	6 19	-65 19	-54 18
C16	272 22	158 20	126 20	-12 17	-80 17	-46 16
C17	282 23	172 21	178 21	11 17	-128 18	-37 17
C18	258 22	120 19	216 21	-19 17	-137 18	-26 17
C19	210 21	143 20	167 20	25 16	-82 17	-4 16
N20	197 17	143 17	165 17	-36 13	17 14	-79 14
N21	167 17	129 17	187 18	-28 13	-28 14	-37 14
N22	181 17	200 17	148 17	-10 14	-9 14	-16 14
N23	191 17	153 17	181 18	-41 14	-42 14	-73 14
O24	306 18	328 18	315 18	-165 14	106 14	-120 15
C25	272 24	199 22	213 22	-58 18	-106 19	-9 18
C26	209 22	206 22	188 22	-55 17	-50 18	-47 17
O27	177 14	174 14	159 14	-30 11	-6 11	-50 12
C28	258 23	166 21	257 24	-42 18	-90 19	-55 18
C29	225 23	235 24	300 26	-127 19	-69 20	13 20
C30	243 24	305 27	229 25	66 20	-11 20	24 21
C31	297 26	429 30	161 23	89 22	-6 20	-107 21
C32	446 30	256 24	257 25	-20 21	-170 22	-139 20
C33	1798 83	270 33	871 50	192 42	-1047 57	-249 33
C34	233 23	219 23	288 25	-31 18	-96 20	-45 19
O35	241 15	167 14	220 16	-11 12	-4 13	-104 12
C36*	187 21	265 24	189 22	-1 18	25 17	-58 18
CL37*	229 6	371 7	343 6	-72 5	-122 5	-19 5
CL38*	232 5	366 6	254 6	-88 5	-67 5	-76 5
CL39*	340 6	306 6	274 6	20 5	76 5	-36 5

Conformation of Heterocycles

In both structures, deviations of ring atoms from a least squares plane through rings B, C and D are on the verge of statistical significance (typically $\leq 0.02 \text{\AA}$). Non-hydrogen atoms directly bonded to one of these rings show deviations of typically $0.05\text{--}0.15 \text{\AA}$ from a least-squares plane through the respective ring.

Ring A is significantly non-planar in both compounds, with puckering amplitudes⁷ of 0.068 in **1** and 0.075 in **2**. In view of the results of the search in the Cambridge Data File⁸ quoted in the preceding communication³, these small puckering amplitudes appear quite reasonable for a five membered ring with four atoms participating in a conjugated system.

Intra- and Intermolecular Hydrogen Bonds

The tautomeric forms of the two compounds and the pattern of intramolecular hydrogen bonds have been determined for **1** and **2** in solution². In fact, synthesis of the two compounds was set about with this pattern of H-bonds in mind, which would render a stable (*E*)-diastereomer².

The NMR-based results² are fully confirmed by the crystal structure analysis (Fig. 1): there are two intramolecular H-bonds in **1** (H 20...N 21 and H 22...N 21), but three intramolecular H-bonds in **2** (H 21...O 27, H 23...N 22, and considerably weaker, H 21...N 22). There can be hardly any doubt that the stability of the (*E*)-isomer is the result of this favourable H-bonding pattern.

In each structure, one acidic hydrogen remains available for intermolecular H-bonding (H 23 in **1** and H 20 in **2**). Since there are several potential H-bond acceptors, the intermolecular H-bonding capabilities are utilized in both structures and they have a dominating influence on the crystal packing (Fig. 5).

In **1**, H 23 forms a H-bond to the carbonyl oxygen O 35 of a molecule related by a center of symmetry (H 23...O 35_{2-x, 1-y, 2-z}, 2.11 Å), leading to the formation of bis-helical centrosymmetric dimers (Fig. 6). Judging from the O...H distance, there is a second, weaker H-bonding interaction of O 35 with H 22 (H 22...O 35_{2-x, 1-y, 2-z}, 2.60 Å).

In **2**, the hydrogen available for intermolecular H-bonding is H 20, which also forms a H-bond with the carbonyl oxygen O 35 of a molecule related by a center of symmetry (H 20...O 35_{2-x, 1-y, -z}, 1.95 Å). This also leads to the formation of centrosymmetric dimers, but of a different kind (Fig. 6). Another H-bond in the crystal structure of **2** involves the solvated chloroform molecule, whose hydrogen interacts with the carbonyl oxygen O 27 (H-C 36...O 27_{1-x, 1-y, 1-z}, 2.35 Å). This is somewhat surprising since O 27 is already involved in at least one intramolecular H-bond, while the carbonyl oxygen atom O 24 is not involved in any hydrogen bonding.

Bonding Geometry

A detailed comparison of the bonding geometry of **1** and **2** with related bilatriene systems will be given in the following communication⁹. Here, we

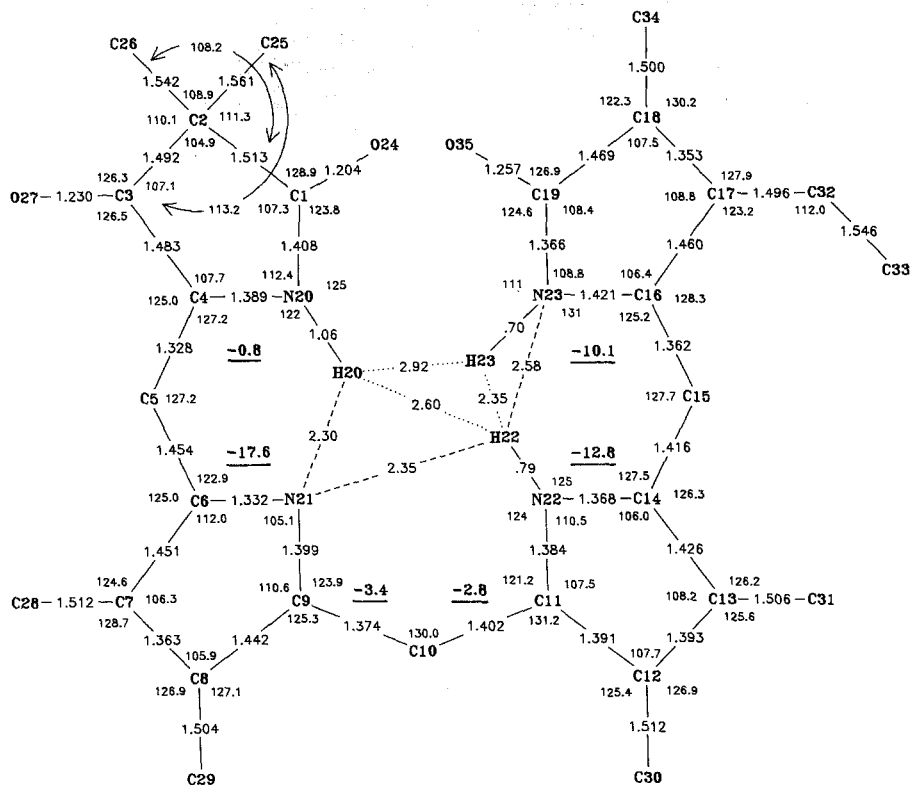
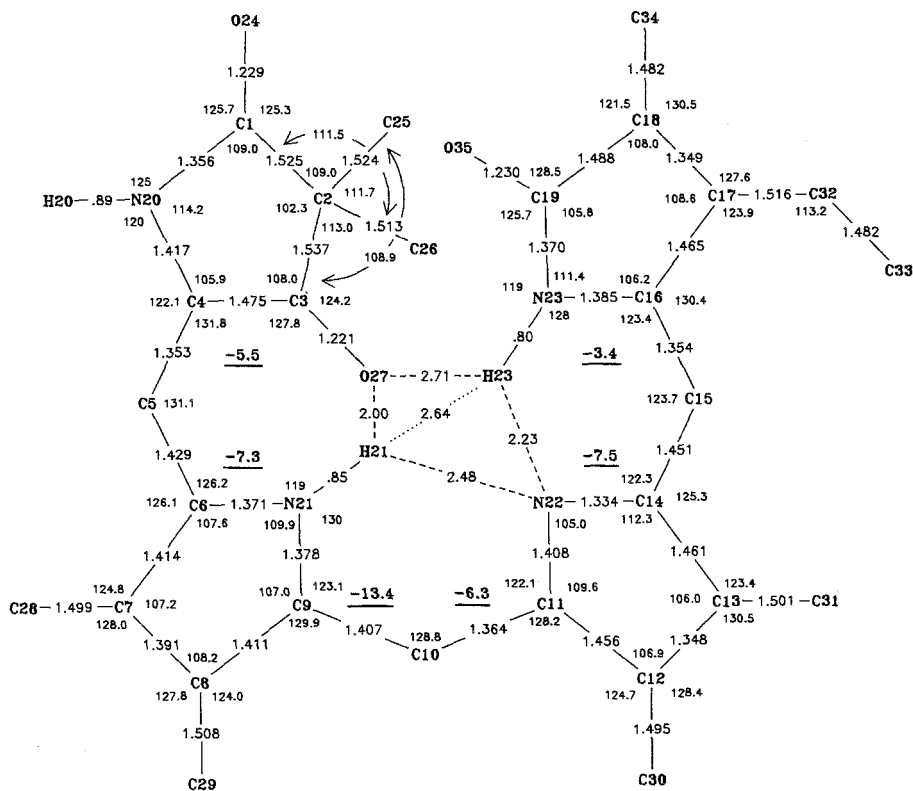


Fig. 1. Calculated bond lengths and bond angles for the low temperatures crystal structures of **1** (left) and **2** (right). Torsion angles about C_m-C_α -bonds are also given (underlined). Derived standard deviations are follows: $1: X-Y, \sigma < 0.009$

will only discuss differences between the two (low temperature) structures. Chemically, they differ “only” with respect to the configuration about one double bond, but this has considerable consequences as far as the stereochemistry and the bonding geometry are concerned.

Many of the differences in bond lengths and bond angles between **1** and **2** are readily explained by the fact that one proton changes from N 22 (in **1**) to N 21 (in **2**). This has the effect, that roughly between atoms C 5 and C 15, the whole bonding geometry of **2** is a mirror image of the geometry of **1**, i.e. rings B and C appear interchanged as far as their bond lengths and angles are concerned. A more complete discussion of this phenomenon will be given in the following communication⁹.

The differences between **1** and **2** observed about rings A and D can partly be understood from the differences in H-bonding and partly from



-0.017 ; N-H, $\sigma \sim 0.05 - 0.09$; X-Y-Z, $\sigma \sim 0.6 - 0.9$; X-N-H, $\sigma \sim 3.9 - 7.1$; **2**: X-Y, $\sigma \sim 0.004 - 0.007$; N-H, $\sigma \sim 0.04$; X-Y-Z, $\sigma \sim 0.3 - 0.5$; X-N-H, $\sigma \sim 1.9 - 2.3$ (X, Y, Z = C, N, O)

the different steric requirements of ring A in the two configurations: in **1**, ring A is “pulled” towards the center of the molecule as a result of the H 20...N 21 interaction, leading to a reduction of the N 20-C 4-C 5 and C 4-C 5-C 6 angles. In **2**, ring A is “pushed” away from the center to accommodate the relatively bulky carbonyl oxygen atom O 27, leading to an “opening up” of the above angles. Ring D—which is not involved in intramolecular H-bonding in **1**—is pulled inwards as a result of the H 23...N 22 H-bond in compound **2**.

Comparison of Room Temperature and Low Temperature Structure of **2**

Fig. 3 shows ORTEP-drawings (50% probability) of the room temperature and low temperature structures of **2**. As observed in the

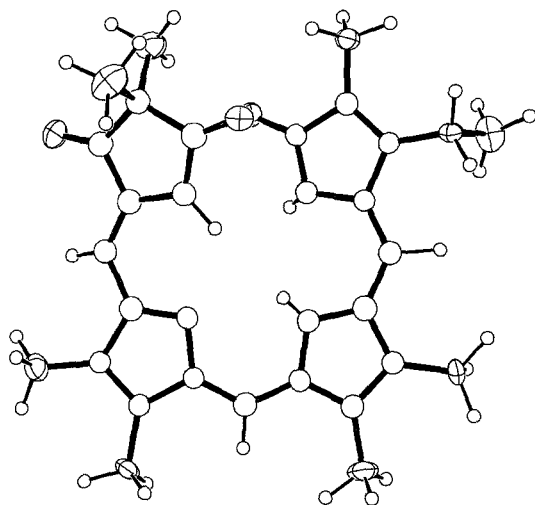


Fig. 2. ORTEP⁵ drawing (50%) of the crystal structure of **1**. Projection approximately into a mean plane through the molecule

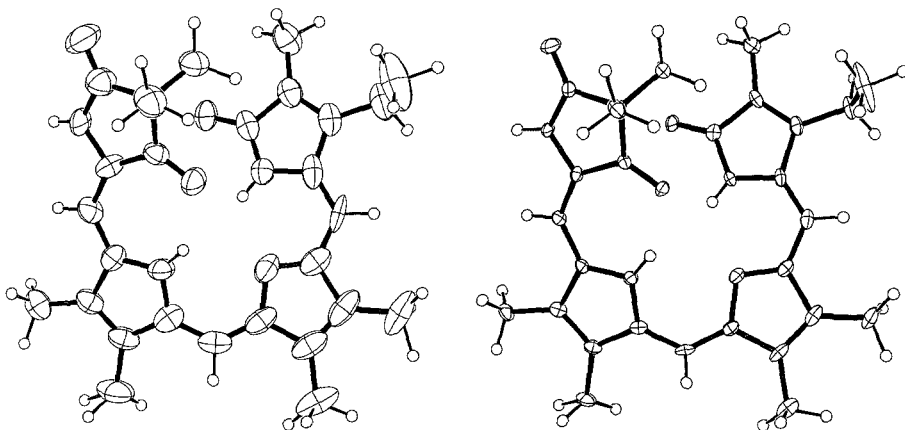


Fig. 3. Room temperature (left) and low temperature (right) crystal structures of **2**: projection approximately into a mean plane

preceding communication³, the room temperature bond lengths are systematically shorter by 0.007 (1) Å than the low-temperature values, which is what one expects as the result of rotational libration.

Fig. 7 shows a scatterplot of room-temperature versus low-temperature u_{ii} values. The dependence expected on the basis of an

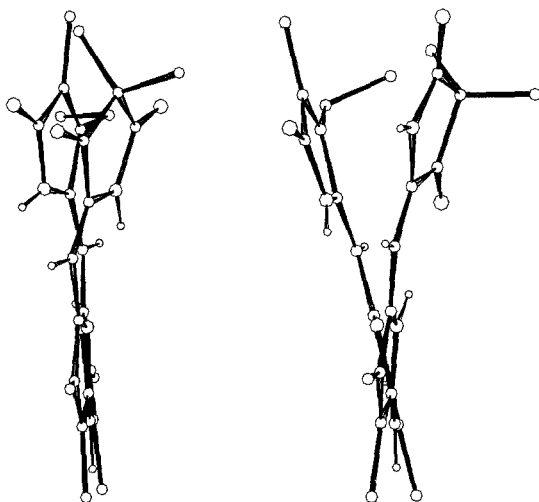


Fig. 4. Projection of **1** (left) and **2** (right) in the direction of the C9–C11 vector

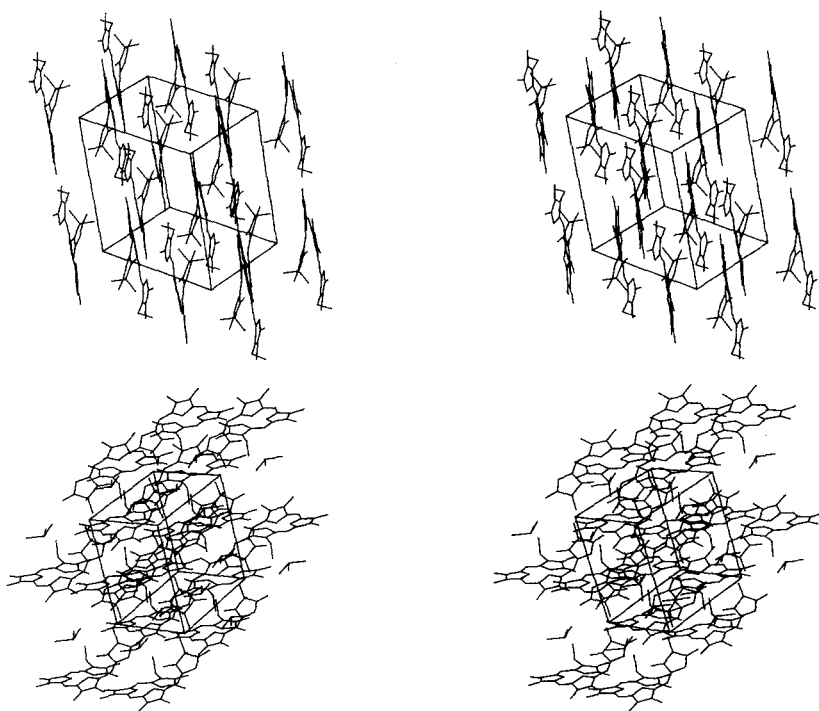


Fig. 5. Packing diagrams for the crystal structures of **1** (top) and **2** (bottom). The directions of the unit cell translations are as follows: **1**: *X* right to left, *Y* left to right, *Z* upwards; **2**: *X* left to right, *Y* upwards, *Z* right to left

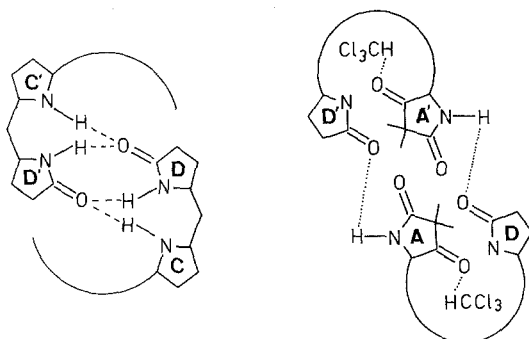


Fig. 6. Schematic representation of the centrosymmetric hydrogen bonded dimers observed in the crystal structures of **1** (left) and **2** (right)

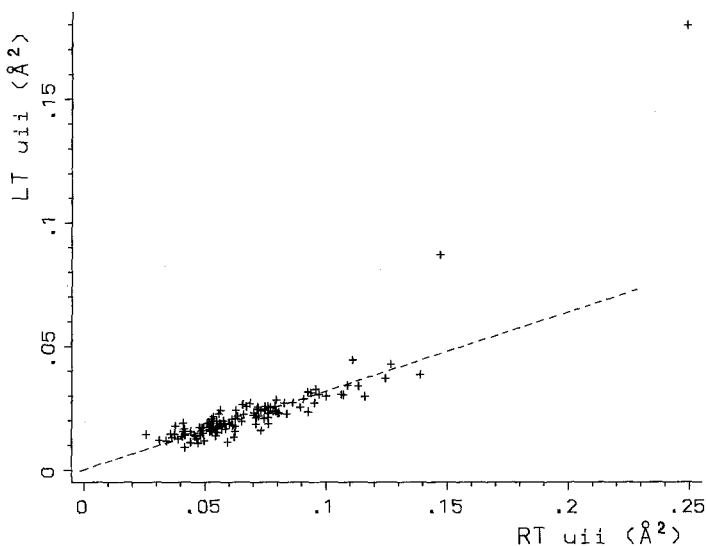


Fig. 7. Scatterplot of room temperature u_{ii} values versus the corresponding low temperature values for the crystal structure of **2**

Einstein-type approximation³ (a line through the origin with slope $T_1/T_2 = 90/293 \approx 0.31$) is also indicated in the plot. While the majority of points is quite compatible with this model, there are two “outliers”, both of which originate from the methyl carbon C 33. This suggests that C 33 librates in a very unharmonic potential, indicating static or dynamic disorder. In fact, the unusual behaviour of C 33 is already evident from inspection of Fig. 3, where its ellipsoid major axis does not change much between the two temperatures.

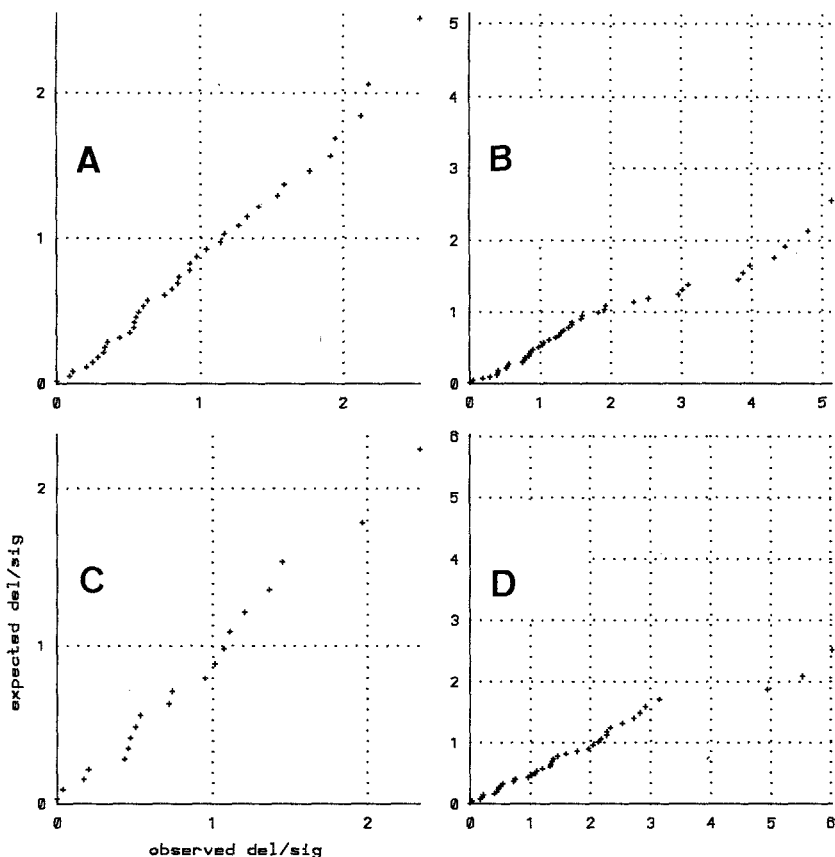


Fig. 8. Halve-normal probability plots for δ_{kl}^3 . *A* k, l = all pairs of bonded atoms; *B* k, l = atoms 1-5, 20, 24-27; *C* $k = 1, 3, 4, 20$; $l = 16-19, 23$; *D* $k = 1-4, 20$; $l = 16-19, 23, 32, 34, 35$

Analysis of Temperature Factors

In the preceding communication³, the observed temperature coefficients were analyzed for indications of molecular flexibility in the crystal. A similar analysis for the structure of **1** is not possible since anisotropic temperature factors are not available for all of its non-hydrogen atoms. For structure **2**, the situation is more favourable.

Judging from the equivalent isotropic temperature coefficients (Table 2), the highest flexibility would be anticipated for the ring A substituents, with considerably smaller u_{iso} values for the substituents of the other rings. This picture is supported by the halve normal probability plots (HNPP).

Fig. 8 A shows the HNPP for δ_{kl} along bond directions, giving no indications of severe systematic errors in the U_{ij} 's. As in the dihydropyromethenones³ there is evidence for internal flexibility within ring A (Fig. 8 B). A HNPP of δ_{kl} values for vectors between ring A and ring D (both rings without substituents; Fig. 8 C) gives no indication of vibrations between the two rings. Analogous results (not shown) are also obtained for the other rings. However, if the substituent atoms of ring D are included, the slope of the corresponding HNPP (Fig. 8 D) decreases significantly. A plausible explanation would be an overall rotational libration of ring D with respect to ring A.

Acknowledgements

C. K. acknowledges support from the *Österreichischer Fonds zur Förderung der wissenschaftlichen Forschung* (Project No. 3736 and 4873), the *Österreichische Akademie der Wissenschaften* and the *Jubiläumsfonds der Oesterreichischen Nationalbank* (Project No. 2214).

References

- ¹ For reviews see: Photomorphogenesis, *Encyclop. Plant Physiol.* **16** (1983).
- ² Falk H., Grubmayr K., Kapl G., Müller N., Zrunek U., *Monatsh. Chem.* **114**, 753 (1983).
- ³ Kratky C., Falk H., Zrunek U., *Monatsh. Chem.* **116**, 607 (1985).
- ⁴ Rüdiger W., *Structure and Bonding* **40**, 101 (1980), and references therein.
- ⁵ Sheldrick G. M., SHELX 76, a program for crystal structure determination, University of Cambridge, England; Stewart G. M., the X-Ray system version of 1976. TR-466, CSS, University of Maryland, U.S.A.; Motherwell S., program PLUTO, University of Cambridge, England; Johnson C. K., ORTEP report ORNL 5138, Oak Ridge National Laboratory, Oak Ridge, Tennessee, U.S.A. (1976).
- ⁶ Kratky C., Jorde C., Falk H., Thirring K., *Tetrahedron* **39**, 1859 (1983); Sheldrick W. S., *Isr. J. Chem.* **23**, 155 (1983).
- ⁷ Dunitz J. D., *X-Ray Analysis and the Structure of Organic Molecules*, Cornell University Press. 1979.
- ⁸ Allen F. H., Kennard O., Taylor R., *Acc. Chem. Res.* **16**, 146 (1983); Kratky C., Bernhard H., *Fakten, Daten, Zitate* **1984** (1), 6.
- ⁹ Kratky C., Falk H., Grubmayr K., Zrunek U., *Monatsh. Chem.* **116**, 761 (1985).
- ¹⁰ Dunitz J. D., *Trans. Amer. Cryst. Assoc.* (in press).